Assessment of weather downtime for the construction of offshore wind farm by using wind and wave simulations

Yuka Kikuchi, Takeshi Ishihara

Department of Civil Engineering, The University of Tokyo, Hongo 7-3-1, Bunkyo-ku, Tokyo, JAPAN

kikuchi@bridge.t.u-tokyo.ac.jp

Abstract. In this study, numerical simulations for winds and waves were carried out using WRF and WW3 and the predicted wind speed, wave height and wave period were validated with measurement. Annual average values of absolute monthly error of wind speed, wave height and wave period were 4.30 %, 12.3 % and 7.8 %. The prediction accuracy were improved by bias modification in the region of low wave height and short wave period. Predicted seasonal frequency distributions showed good agreement with measurements. The criteria of experienced construction methods were investigated at Choshi and Kitakyushu wind farm and the sensitivity of environmental conditions on weather downtime were clarified. At Choshi, the weather downtime was predicted by using wind and wave simulations and showed good agreement with the actual weather downtime.

1. Introduction

In the construction of offshore wind farm, the assessment of weather downtime is important. Each work vessel and construction method have criteria for wind speed, wave height and wave period. For the construction, wind and wave conditions should be less than the criteria for several hours.

Conventionally, weather downtime was estimated from met ocean statistics in the form of exceedance curves, monthly means or non-exceedance persistence tables [1-4], but these data do not consider the sequential nature of marine engineering projects. Then, sequenced downtime analysis has been applied by using a time-domain simulation of a sequence of tasks within a long time series of met ocean data [5-8]. For a successful application of the SDA technique, an accurate time-series of wind and wave data is required. B. J. Beamsley et al. [5] built the hindcasting system comprising of a coupled WW3 / SWAN / POM / WRF (Wave Watch III / Simulating Waves Nearshore / Princeton Ocean Model / the Weather Research and Forecasting Model) in their weather downtime calculator for offshore engineering activities. In Japan, Ishihara et al [9] used RAMS (Regional Atmospheric Modeling System) and SWAN for the predictions for weather downtime assessment of offshore wind farm construction. However, wave period predicted by SWAN overestimated the measurement and the validation was performed only with near-shore measurement. Furthermore, the criteria was unknown, since there was no construction results of offshore wind farm in Japan at that time.

Meanwhile, the prediction accuracy of simulations have been improved. Fukushima and Ishihara [10] clarified that the complex land use and elevation had a large effect on the prediction accuracy of offshore wind speed. Tanemoto and Ishihara [11] proposed combined typhoon and mesoscale model to improve the prediction accuracy of wave height in tropical cyclone area. Also, in 2012, two wind farms were constructed at Choshi and Kitakyushu in Japan as national demonstration projects [12]. Choshi is on the East coast in Japan, facing the Pacific Ocean, where high wave height and swell is

typical. Kitakyushu is on the West coast in Japan, facing Japan Sea, where the low wave height is typical. Here, wind and wave measurement data have been obtained with meteorological masts.

In this study, the prediction accuracy of the latest wind and wave simulations was validated with measurement data at Choshi wind farm. Then, the prediction accuracy was improved by bias correction for low wave height and short wave period. Seasonal frequency distributions of wind speed, wave height and wave period were assessed. Finally, experienced construction methods and criteria were investigated at Choshi and Kitakyushu wind farm and the sensitivity of environmental conditions on weather downtime was investigated. The weather downtime was predicted by using the predicted wind and wave simulations and validated with the actual construction results.

2. Wind and wave simulation and measurement

In this section, wind and wave simulations and measurements are described. Offshore wind simulations were performed with Weather Research and Forecasting (WRF) Ver. 3.4 [13] model. The model configuration and domain are shown in Figure 1 and Table 1. Horizontally, the 1800 km × 1800 km domain was set at 18 km resolution, and subsequently nesting at 6 km and 2 km resolution. Geographical Survey Institute 50 m resolution data and National Land Information Division 100 m resolution data were used for elevation and land use in order to reproduce the effect of complex terrains. OSTIA (Operational Sea Surface Temperature and Sea Ice Analysis) was used for sea surface temperature data in order to reproduce the effect of sea surface temperature. Please see the simulation detail in reference [10].

Offshore wave simulations were performed with Wave Watch III (WW3) Ver. 3.14 [14]. The model configuration and domain are shown in Figure 2 and Table 2. The higher resolution wind field simulations were obtained running WRF at 18 km resolution and subsequently nesting at 6 km and 2 km resolution. The initial and boundary conditions for the 18 km model corresponds to the NCEP-FNL predictions with 1.0º or NNRP predictions with 2.5º. The size of Domain 1 was set as large enough to reproduce the swell in Pacific Ocean. Tropical cyclone has a significant effect on wave climate in Japan, and so combined typhoon and mesoscale wind field model proposed by Tanemoto and Ishihara[11] is used. In the model, wind speeds u_C is predicted by combining predicted wind speed by mesoscale model u_M and that predicted by tropical cyclone model u_T with the following equation.

$$u_C = Wu_T + (1-W)u_M \tag{1}$$

$$W = \left(\frac{R_{\mathbf{B}}^2 - r^2}{R_{\mathbf{B}}^2 + r^2} \right)^{0.5} \qquad (R_B \succ r) \tag{2}$$

Here r is the distance from the center of a tropical cyclone, and R_B is the tropical cyclone outside boundary. Please see the simulation detail in reference [11]. In this study, significant wave height H_s and significant wave period T_s are calculated by the following equations. Here $E(f,\theta)$ is energy spectrum for frequency f and direction θ.

$$H_s \approx 0.965 H_{m0} = 0.956 \times 4\sqrt{m_0} \;, \qquad T_s \approx T_{m-1,0} = \frac{m_{-1}}{m_0} \tag{3}$$

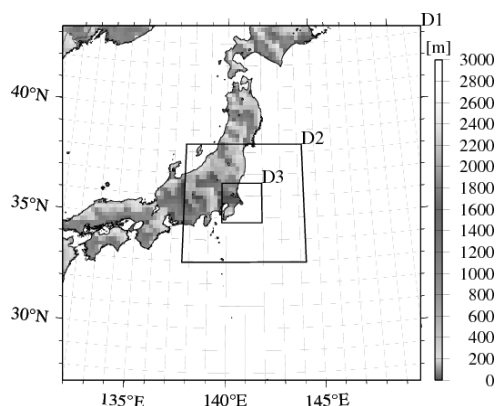$$m_n = \iint f^n E(f,\theta)\,df\,d\theta \tag{4}$$
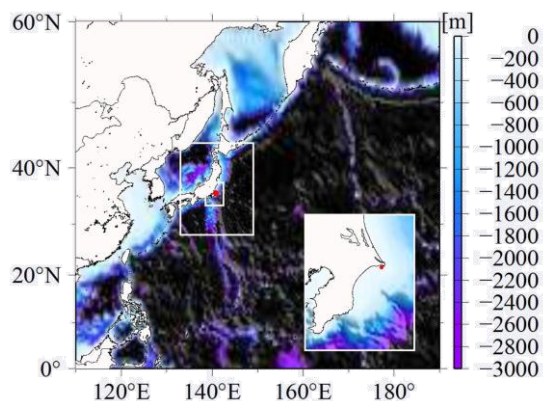
Figure 1. WRF domain.

Figure 2. Wave Watch III domain.

Table 1. WRF parameters and schemes.

	Domain 1	Domain 2	Domain 3
Calculation time	2013.2 – 2014.1		
Spin-up	More than 10 days		
Domain	133º-149ºE,28.0º-44.0ºN	138.5º-142.5ºE,33.5º-37.5ºN	139.7º-141.3ºE,34.7º-36.3ºN
Vertical resolution	45 levels (Surface to 50 hPa)		
Horizontal resolution	18km (100 × 100 grids)	6km (100 × 100 grids)	2km (100 × 100 grids)
Meteorological data	NCEP-FNL 1º×1º 6-hourly		
Sea surface temperature	OSTIA 0.05º×0.05º 6-hourly		
Geographical data	Elevation: Geographical Survey Institute 50m Landuse: National Land Information Division 100m		
Time step	72s	24s	8s
Microphysics scheme	Ferrie (new Eta) microphysics scheme		
Planetary boundary layer	Mellor-Yamada-Janlic TKE level2.5 scheme		
Surface layer	Monin-Obukhov (Janjic Eta) scheme		
Land surface	Unified Noah land surface scheme		
4DDA	Grid nudging (excluding domain 3)		

Table 2. WW3 parameters and schemes.

	Domain 1	Domain 2	Domain 3	Domain 4
Calculation time	2013.2 – 2014.1			
Spin-up	More than 10 days			
Horizontal resolution	0.5º×0.5º (161×121 grids)	0.2º×0.2º (81×81 grids)	0.05º×0.05º (81×81 grids)	0.02º×0.02º (81×81 grids)
Domains	110º-190ºE, 0.0º-60.0ºN	133º-149ºE, 28.0º-44.0ºN	138.5º-142.5ºE, 33.5º-37.5ºN	139.7º-141.3ºE, 34.7º-36.3ºN
Bathymetry	ETOPO2		ETOPO1	
Sea surface boundary	NCEP-FNL(1.0º) Or NNRP(2.5º)	WRF(18km)	WRF(6km)	WRF(2km)
Lateral boundary	Open	Nest down (2-way nesting)		
Spectrum resolution	36 directions and 36 frequencies (0.0345~0.97Hz)			

At Choshi wind farm, a met mast has been installed 285 m east to the wind turbine and equipped with cup anemometers at eight different heights, sonic anemometers at three different heights and a Doppler LIDAR. In addition, sea surface temperature is measured at the tower. In this study, 10-minute average wind speed measured by the Doppler LIDAR was used for validation. The data in west direction (258.75°~281.25°) was not used due to the wake effect of wind turbine. In September and October, sonic anemometers data was used due to the missing of Doppler LIDAR.

Ultrasonic wave detector has been installed at the sea bed between turbine and met mast. In this study, 20-minute significant wave heights and significant wave periods measured by Ultrasonic Wave Detector were used for validation.

The wind and wave measurement data was summarized in Table 3. The met mast measurement started from February in 2013 and ultrasonic wave detector measurement started from January 2010.

Table 3. Wind and wave measurement data.

Wave	Observation period	2013.2-
	Location	N35°53'55″ E140°45'14″
	Water depth	15m
	Measuring instrument	Ultrasonic Wave Detector
	Averaging time	20min.
Wind	Observation period	2010.1-
	Location	N35°44'18″ E140°51'24″
	Observation height	80m
	Measuring instrument	Lidar Vane (in Sep. and Oct.)
	Averaging time	10min

3. Validation of wind and wave simulations

3.1. Prediction of monthly average value of wind speed, wave height and wave period

Wind and wave simulation has been conducted from Feb. 2013 to Jan. 2014. The prediction accuracy of wind and wave simulation was evaluated with relative error with monthly average of simulation X_s and that of measurement X_o.

$$\gamma = (X_s - X_o)/X_o \qquad (5)$$

Figure 3 showed time series of measured and predicted wind speed at the height of 80 m, significant wave height and significant wave period in July and January as typical month of summer and winter. Figure 4 and Table 4 showed monthly average value of those. The standard deviation of predictions are important, but it will be discussed in future study.

Predicted wind speed in July reproduced high wind speed well and showed good agreement with measurements. That in January reproduced three days cycle of high wind speed well. Its relative error ranged from -2.7% to 9.3% and annual average value of absolute monthly error was 4.30 %. The higher relative error in winter was due to the difference of sea surface temperature between OSTIA and measurement data as reference [10] showed.

Predicted significant wave height in July reproduced low wave height due to swell and high wave height due to the front. That in January reproduced periodic variation of high wave height well. However, the significant wave height less than 1 m underestimate the measurement. Its relative error ranged from -27.7 % to 13.3 % and annual average value of absolute monthly error was 12.3 %. The relative error was higher in winter since the reproducibility of high wave height in low pressure was not good.

Predicted significant wave period in July reproduced long wave period due to swell. That in January matched with measurement. However, the significant wave period around 6 sec underestimated the measurement. Its relative error ranged from -15.9 % to 6.9% and annual average value of absolute monthly error was 7.8 %. Monthly average of prediction reproduced that of measurement well, but the error in July showed higher value.

The underestimation of wave height less than 1 m and wave period around 8 sec. has a large effect on the estimation of weather downtime, since the construction criteria is usually set to around 1m of wave height and 8 sec of wave period. Then, the seasonal frequency distributions were investigated and the underestimation was evaluated precisely in the next section.
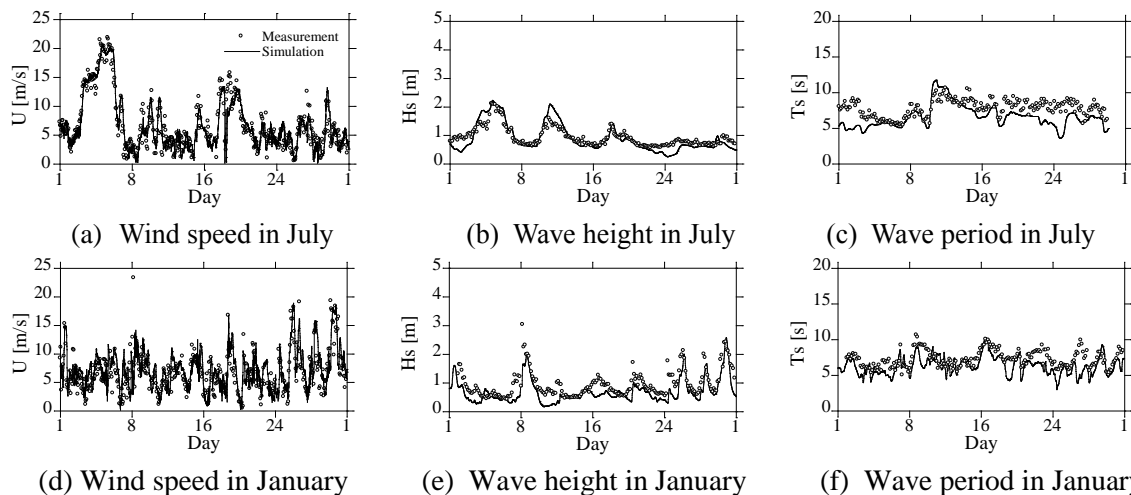

| (a) Wind speed in July | (b) Wave height in July | (c) Wave period in July |
| (d) Wind speed in January | (e) Wave height in January | (f) Wave period in January |

Figure 3. Comparison between measured and predicted wind speed, wave height and wave period.

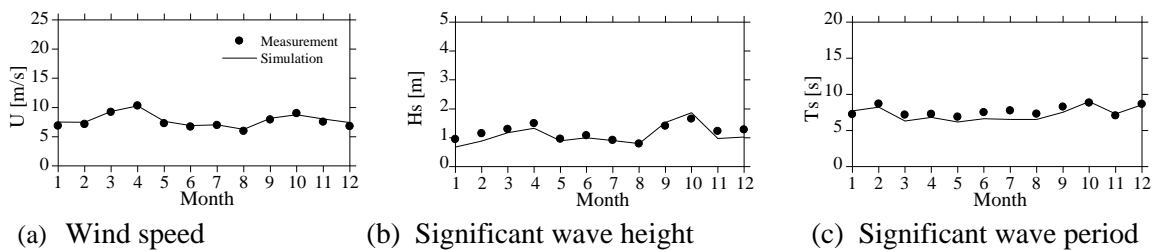| (a) Wind speed | (b) Significant wave height | (c) Significant wave period |

Figure 4. Comparison of measured and predicted monthly average of wind speed, wave height and wave period.

Table 4. Relative error of measured and predicted monthly averaged value and these absolute average (%) of wind speed U, significant wave height Hs and significant wave period Ts.

Mon.	1	2	3	4	5	6	7	8	9	10	11	12	Ave.
U	4.4	1.6	0.3	4.9	2.7	1.7	5.2	3.2	-2.7	7.1	8.8	9.3	4.3
Hs	-27.7	-22.9	-9.2	-11.1	-6.07	-6.6	-1.4	1.3	8.6	13.3	-20.0	-19.1	12.3
Ts	6.9	-5.3	-11.8	-6.2	-9.9	-11.3	-15.9	-10.7	-8.9	2.0	3.2	-0.9	7.8

3.2. Prediction of seasonal frequency distributions

Seasonal frequency distributions of measured and predicted wind speed, significant wave height and significant wave period were evaluated as shown in Figure 5. About wind speed, measured seasonal frequency distributions (expressed as dot in Fig. 5) showed that the occurrence time of wind speed less than 10 m/s were 20~25 days per month in all seasons. It meant that wind speed has less effect on seasonal variation of weather downtime. Predicted seasonal frequency distributions (expressed as thin line in Fig. 5) agreed well with measured one, but underestimated it in winter since the predicted wind speed overestimate the measurement as described in the previous section.

About wave height, measured seasonal frequency distributions showed that occurrence time of wave height less than 1.0 m was under 15 days per month in spring and autumn, 15 days in winter, and 20 days in summer. It showed that wave height had a large effect on seasonal variation of weather downtime. Predicted occurrence time of wave height less than 1.0 m overestimated the measurement in all seasons, due to the underestimation of wave height as shown in the previous section. In winter, predicted occurrence time of wave height above 1.0 m overestimated the measurement, since the prediction underestimated the measurement of wave height less than 1.0 m as described in the previous section.

About wave period, measured seasonal frequency distribution showed that the occurrence time of wave period less than 8.0 sec was around 15-20 days in all seasons. It showed that wave period has less effect on seasonal variation of weather downtime. Predicted occurrence time of wave period less than 8.0 sec overestimated the measured one in all seasons, since the prediction underestimated the measurement of wave period less than 8.0 sec as described in the previous section.

The underestimation of wave height less than 1.0 m and that of wave period less than 8.0 sec had a big effect on the assessment of weather downtime since the construction criteria were around these values. Then, the biases of wave height and wave period were evaluated as Figure 6 showed. Bins were set 0.25 m for wave height and 1 sec for wave period. The investigated bias were modelled with linear equation by least square method as the following equation.

$$\beta_{Hs} = 0.16 H_{s,\,pred} - 0.25 \tag{6}$$

$$\beta_{Ts} = 0.34 T_{s,\,pred} - 3.01 \tag{7}$$

The predicted wave height and wave period was modified with following equations.

$$H_{s,\,mod} = H_{s,\,pred} - \beta_{Hs} \tag{8}$$

$$T_{s,\,mod} = T_{s,\,pred} - \beta_{Ts} \tag{9}$$

The averaging time difference between simulation and measurement was also modified following the method in reference [15]. The modified wave heights and wave periods improved their annual relative error of wave height from 12.3 % to 9.9 % and that of wave period from 7.8 % to 2.9 % for wave period. The quality of this bias correction method should be discussed in future research.

Measured and modified predicted seasonal frequency distributions (expressed as thick line in Fig. 5) showed a good agreement in all seasons. Prediction accuracy of occurrence time of significant wave heights less than 1.0 m and that of significant wave period less than 6.0 sec improved modification, but that of occurrence time of significant wave period less than 8.0 sec had still some overestimation.
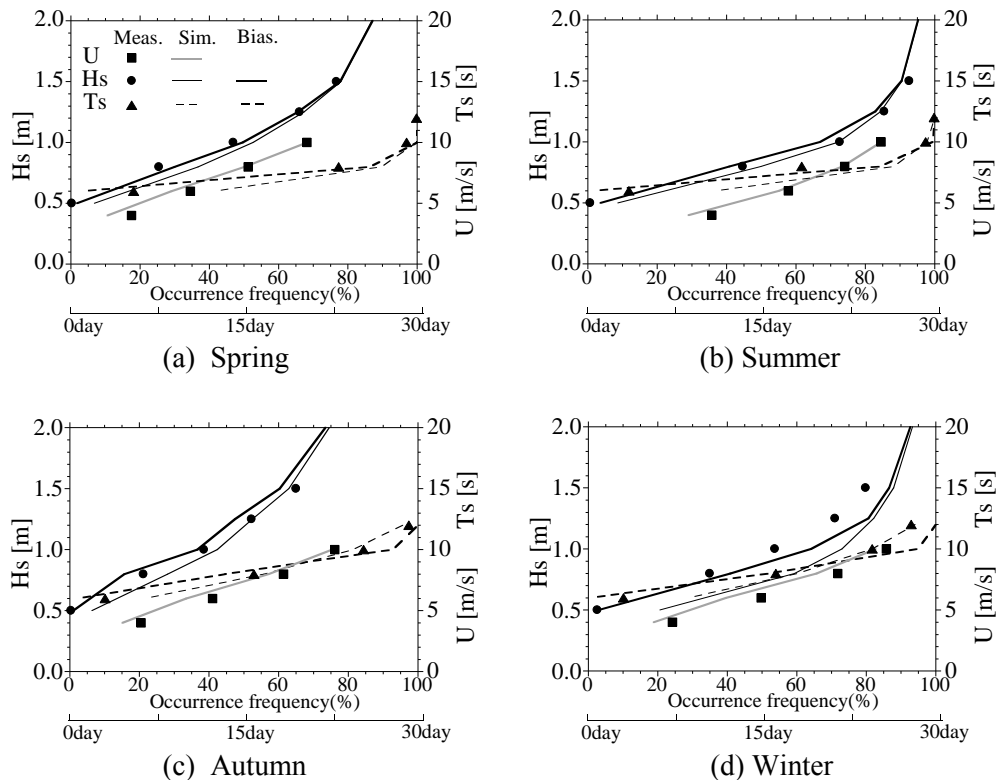
Figure 5. Comparison of seasonal frequency distribution of wind speed, significant wave height, and significant wave period among measurements, predictions and modified predictions.
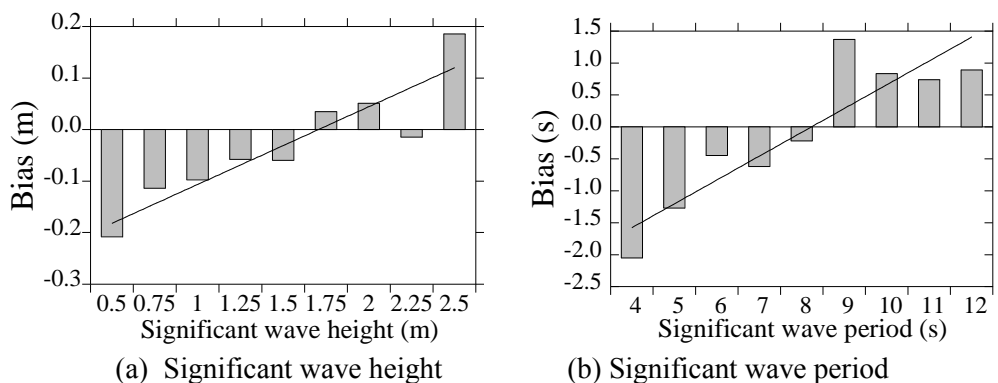

Figure 6. Bias of predicted significant wave height and significant wave period.

4. Assessment of weather downtime by using simulations

4.1. Sensitivity of environmental conditions on weather downtime.

In this section, a sensitivity of environmental conditions on weather downtime was investigated at Choshi and Kitakyushu wind farms. Both wind farms were constructed as national demonstration projects in 2012. At Choshi site, 2.4 MW wind turbine were installed with concrete gravity type foundation, 3.1 km far away from the coast at 11.9 m water depth. At Kitakyushu site, 2 MW wind turbine was installed with jacket type foundation, 1.3 km far away from the coast at 14 m water depth.

The hind cast of wave height and wave period in Choshi and Kitakyushu were investigated as Figure 7 showed. Choshi is facing the Pacific Ocean where the high wave height and swell is typical, whereas Kikakyushu is facing Japan Sea where the low wave height is typical. The average of

significant wave height is 1.24 m at Choshi and 0.67 m at Kitakyushu. Probability of occurrence of wave height less than 1 m wave height is 0 % at Choshi, while 80.40 % at Kitakyushu. The average of significant wave period is 8.13 sec at Choshi and 4.93 sec at Kitakyushu. Probability of occurrence of wave period less than 8 sec is 99 % at Kitakyushu and 57 % at Choshi.

Construction methods and their criteria were investigated at the two wind farms. Table 5 summarised them as Method 1 and Method 2. Construction was categorised into three main works: bottom preparation, installation of substructure and installation of wind turbine. For bottom preparation, Method 1 employed submerged backhoe method, which has less effect of wave height. Method 2 employed weight free falling base levelling with floating crane, which required the horizontal accuracy. The construction method was decided by wave climate. For installation of substructure, both methods employed floating crane. Method 1 used 1600 t crane and Method 2 used 3700 t crane. The size was chosen by the substructure weight. For installation of wind turbine, both methods employed self-elevated platform, but it was found that the construction criteria was driven by the access method to SEP. Method 1 employed hanging move method with basket which allows high wave height, but Method 2 employed ladder. The criteria was also decided by wave climate as bottom preparation. The result was implied that the work criteria were decided by wave climate and the weight of equipment.

Figure 8 showed the predicted workability at Choshi and Kitakyushu by using investigated criteria and measured wind speed, wave height and wave period at the two sites. Here, workability was defined as the ratio of workable days (the time other than weather downtime) into whole construction days. The construction period and the condition of workable day followed the definition in the following section. The workability at Choshi has high dependency on the construction methods, but that at Kitakyushu has it less. It was clarified that severe wave condition has high sensitivity of construction methods on workability.
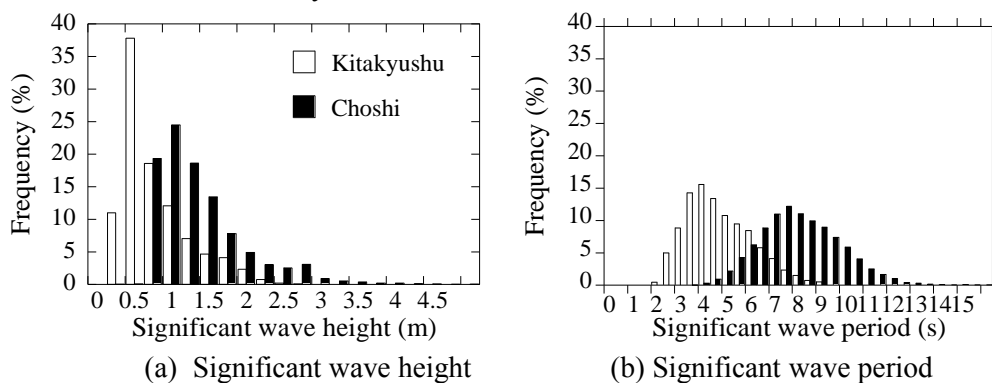

(a) Significant wave height　　　　　(b) Significant wave period

Figure. 7 Frequency of wave height and wave period at Choshi and Kitakyushu.

Table 5. Method for constructing bottom-up offshore wind farm.
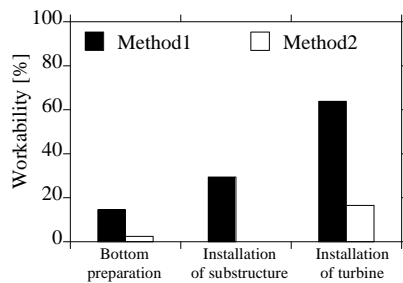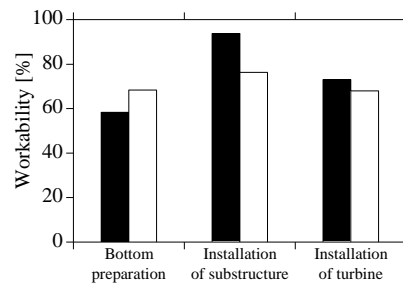
	Construction method 1	Construction method 2
Bottom preparation	$Hs \leqq 1$ m Required duration: several hours in daytime Submerged backhoe Source: Shibuya Diving Industry, Co [17].	$Hs \leqq 0.8$ m for several hours Required duration: several hours in daytime Weight free falling base leveling With floating crane[16] Source: NEDO[12]

Table 5 (Continuous). Method for constructing bottom-up offshore wind farm.

Installation of substructure	$Hs \leqq 1.25$ m, $Ts \leqq 8.0$ s Required duration: 36 hours Floating crane Shinsho-1600 Source: Kajima Corporation[18]	$Hs \leqq 0.5$ m Required duration: several hours in daytime Floating crane Musashi-3700 Source: NEDO[12]
Installation of wind turbine	$Hs \leqq 2.5$ m, $U \leqq 10$ m/s ($U \leqq 8$ m/s for installing blades) Required duration: several hours in daytime Basket Source: Kajima Corporation[18]	$Hs \leqq 1$ m, $U \leqq 10$ m/s ($U \leqq 6$ m/s for installing blades) Required duration: several hours in daytime Access vessel Source: NEDO[12]

(a) Choshi   (b) Kitakyushu
Figure 8. Workability by construction Method 1 and Method 2.

4.2. Prediction of weather downtime by using wind and wave simulations

Workability was assessed by using wind and wave simulations and validated at Choshi where workability has a high sensitivity to construction method. Table 6 showed the experienced workability at Choshi wind farm. Here, workability was defined as the ratio of workable day to all construction day. The workable day was defined as the day when the workable condition continue more than 12 hours during daytime from 6:00 to 18:00 for the bottom preparation and the installation of wind turbine, and as the day when workable condition continue more than 36 hours for the installation of substructure. The workable condition indicates that the wind and wave was under the thresholds as Table 5 showed.

By using wind and wave measurement data, workability was assessed. The construction period and workable days were set as same as Choshi. It was assumed that the work continued when the exceedance time was less than 20 minutes. For wind measurement data, the nearest observation mast data was converted to the site, since the met mast was not yet installed at the construction period. The

validation of its conversion was confirmed at reference [15]. Figure 9 showed the workability experienced (expressed as dot) and predicted by measurement (expressed as hatched bar). Evaluated workability showed a good agreement with the experienced one, which validated the investigated construction criteria.

Then, workability was predicted by using wind and wave simulations in the same way as using measurement data as Figure 9 showed (expressed as black bar). The predicted workability by using simulations showed a good agreement with that by measurement. It was clarified that workability was assessed well with high accurate wind and wave simulations and appropriate construction criteria.

Table 6. Workability at Choshi offshore wind farm.

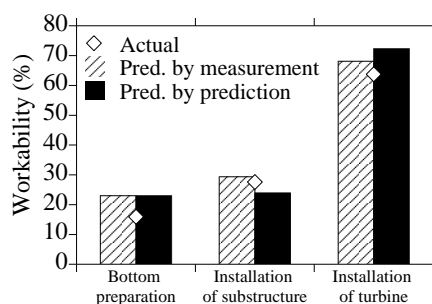| Work	Period	Workability
Bottom preparation	2012/2/23-2012/4/6	15.9% (7/44day)
Installation of substructure	2012/6/12-2012/7/10	27.6% (8/29day)
Installation of turbine	2012/9/9-2012/10/25	63.8% (30/47day)

Figure 9. Workability experienced and predicted by measured and simulated environmental condition.

5. Conclusions

In this study, weather downtime for the construction of offshore wind farm was assessed by using wind and wave simulations. The conclusions were summarized as follows.

1) The predicted wind speed, wave height and wave period reproduced the characteristic of low wind speed and wave height in summer and high wind speed and wave height in winter. Annual average values of absolute monthly error were 4.30 %, 12.3 % and 7.8 %, respectively.
2) The prediction accuracy was improved by bias corrections in the region of low wave height and short wave period. Predicted seasonal frequency distributions of wind speed, wave height and wave period showed good agreement with measurements.
3) The assessed weather downtime by using predicted wind speed, wave height and wave period and the investigated criteria showed good agreement with actual weather downtime at Choshi.

References

[1]   Graham C 1982 The parameterisation and prediction of wave height and wind speed persistance statistics or oil industry operational planning purposes *Coastal Eng.* **6** pp303-29
[2]   Anastasiou K and Tsekos C 1996 Operability analysis of marine projects based on Markov theory *Applied ocean research* **18** 329-52
[3]   Van der Wal R J and de Boer G 2004 Downtime analysis techniques for complex offshore and dredging operations *Proc. Int. Conf. on Offshore Mechanics and Arctic Engineering (Vancouver)* vol 2 (New York: United States/American Society of Mechanical Engineers) pp 93-101
[4]   Sheu M N, Matha D and Muskulus M 2012 Validation of a Markov-based Weather Model or simulation of O&M for ofshore wind farms *Proc. Int. Con. On Offshore and Polar Engineering Conference (Rhodes)*
[5]   Beamslye B J, McComb P, Johnson D, and Silk J 2007 Estimatimg weather downtime for ocean engineering using sequential downtime analysis (SDA) *MetOcean Solutions Limited Technical Paper*
[6]   Dewan A, Asgarpur M and Savenjie R 2015 Commercial proof of innovative offshore wind installation concepts using ECN Install Tool *ECN Technical paper ECN-E—15-007*
[7]   ABPmer 2016 Accounting for weather in marine operations − analysing the past to inform future decisions *ABPmer thechnical report*
[8]   ABP mer 2011 SEASTATES the metocean forecase service from ABPmer *ABPmer thechnical report*
[9]   Ishihara T, Yamaguchi A, Sarwar M W and Oikawa S 2012 Numerical study of wave and wind conditions and weather window for construction of offshore wind power plants *Journal of Wind Energy, JWEA*, **35** pp 7-14
[10]   Fukushima M, Yamaguchi A and Ishihara T 2014 Offshore wind speed prediction by using mesoscale model, *Proc. Int. Con. on Grand Renewable Energy 2014* (Tokyo)
[11]   Tanemoto J and Ishihara T 2014 Extreme wave height prediction by using combined wind field of mesoscale and typhoon model, *Proc. Int. Con. on Grand Renewable Energy 2014* (Tokyo)
[12]   New Energy and Industrial Technology Development Organization 2016 NEDO Offshore bottom-up wind farm demonstration project (In Japanese), http://www.nedo.go.jp/fuusha/index.html, Accessed in 2016. 6.
[13]   Skamarocj W C, Klemp J B, Dudhia J, Gill D O, Barker D M, Duda M G, Huang X, Wang W, and Powers J G 2009 A description of the advanced research WRF version 3 *NCAR Technical Note 276*
[14]   Tolman H L 2009 User manual and system documentation of WAVEWATCH III version 3.14 *NOAA/NWS/NCEP/MMAB Technical Note 276*
[15]   Ishihara T and Yamaguchi A 2015 Prediction of the extreme wind speed in the mixed climate region by using Monte Carlo simulation and Measure-Correlate-Predict method *Wind Energy* **18** pp171-186
[16]   Penta-Ocean Construction Co. LTD 2014 Installation of offshore wind turbine in Kikakyushu (In Japanese) *Workvessel* **314** pp13-8
[17]   Shibuya diving industry Co. HP of shibuya diving industry 2016 Submerged backhoe (In Japanese), http://www.shibuya-diving.co.jp/technology.html Accessed in 2016. 6.
[18]   Kajima Coorporation 2016 Installation of the first bottom-up offshore wind turbine in Japan at Choshi (In Japanese), http://www.kajima.co.jp/news/press/201302/27c1-j.htm, Accessed in 2016. 6.